# *Articles*

## Crystal Engineering of Rare Earth Amides: $^3_\infty$[Tb(Im)$_3$]@NH$_3$, a Homoleptic 3D Network Exhibiting Strong Luminescence

Klaus Müller-Buschbaum,*,† Sonja Gomez-Torres,† Patrick Larsen,‡ and Claudia Wickleder‡

*Institut für Anorganische Chemie, Universität zu Köln, Greinstrasse 6, 50939 Köln, Germany, and Anorganische Chemie, Universität Siegen, 57068 Siegen, Germany*

*Received August 24, 2006. Revised Manuscript Received November 28, 2006*

The solvent-free reaction of terbium metal with an imidazole melt ($C_3H_4N_2$, ImH) yields single-crystalline $^3_\infty$[Tb(Im)$_3$]@NH$_3$ (Im$^-$ = $C_3H_3N_2^-$, imidazolate anion) and hydrogen. Both N atoms of the imidazolate rings coordinate $\eta^1$ to terbium cations, thereby forming a homoleptic three-dimensional network. The $Tb^{3+}$ ions exhibit complete nitrogen coordination, resulting in trigonal prisms as coordination polyhedra and C.N. = 6. The network contains cavities large enough to take up $NH_3$ molecules, the latter formed by the partial decomposition reaction of the amine ligand in the melt reaction. Ammonia can be removed thermally or over time without decomposition of the network. Unsubstituted imidazole can thus be utilized for crystal engineering and the formation of rare earth amide network structures. The compound exhibits an amazingly strong green emission. The emission spectrum shows the typical $Tb^{3+}$ f−f transitions; additionally, an efficient ligand → $Tb^{3+}$ energy transfer is observed.

### Introduction

The systematic study of aromatic *N*-heterocyclic amines in direct redox reactions with rare earth metals gives an overview on the variety of coordination modes of these ligands concerning number and position of coordinating N atoms, the coordination numbers and valences of the lanthanide ions as well as the dimensionality of the products obtained.[1] Solvent-free reactions show a general trend toward coordination polymers[1−6] in carbazolates,[2,3] pyrazolates,[4,5] and benzotriazolates,[6] whereas additional substituents on the amine ligands prevent polymerization.[7−14] For imidazole, e.g., the *N*-methyl substituted ring is a system known for rare earth complexation.[7−9] Substitution at the N atom blocks this coordination site so that no linking is possible, resulting in a single $\eta^1$ coordination mode. Sterically active substituents like $^t$Bu, Ph,[10−12] or even coordinating pyridyl rings[13,14] also prevent dimensional structures. Recently, we have shown that the 3*N*-heterocycle 1,2,4-triazole in $^3_\infty$[Yb(Tz)$_3$] and $^3_\infty$[Eu$_2$(Tz)$_5$(TzH)$_2$], Tz$^-$ = triazolate anion, TzH = 1,2,4-triazole[15] as well as imidazole in $^3_\infty$[Pr(Im)$_3$(ImH)]@ImH[16] are able to build up three-dimensional structures. So far, these are the only examples of network structures of rare earth amides. With $^3_\infty$[Tb(Im)$_3$]@NH$_3$, we now present a novel network that illustrates the influence of the smaller $Tb^{3+}$ ion compared to $Pr^{3+}$[16] in imidazolates as well as its outstanding luminescence properties. The compound is of interest from a materials point of view because of the possibility of removing the ammonia molecules without decomposition of the network and thus tailoring the properties, e.g., color rendering or energy-transfer rate, and thereby the luminescence efficiency.

### Experimental Section

**Synthesis of $^3_\infty$[Tb(Im)$_3$]@NH$_3$.** In general, all manipulations were carried out under inert atmospheric conditions using a glove box, ampule, and vacuum line techniques. Heating furnaces were equipped with $Al_2O_3$ tubes and EUROTHERM 2416 control elements. Hg (Riedel-de-Haen) of 99.99% purity was used for

† Universitat zu Koln.
‡ Universitat Siegen.

(1) Müller-Buschbaum, K. *Z. Anorg. Allg. Chem.* **2005**, *631*, 811
(2) Müller-Buschbaum, K.; Quitmann, C. C. *Z. Anorg. Allg. Chem.* **2003**, *629*, 1610.
(3) Müller-Buschbaum, K.; Quitmann, C. C. *Eur. J. Inorg. Chem.* **2004**, 4330.
(4) Quitmann, C. C.; Müller-Buschbaum, K. *Z. Naturforsch.* **2004**, *59b*, 562.
(5) Quitmann, C. C.; Müller-Buschbaum, K. *Z. Anorg. Allg. Chem.* **2005**, *631*, 1191.
(6) Müller-Buschbaum, K.; Mokaddem, Y. *Eur. J. Inorg. Chem.* **2006**, 2000.
(7) Evans, W. J.; Rabe, G. W.; Ziller, J. W. *Inorg. Chem.* **1994**, *33*, 3072.
(8) Evans, W. J.; Rabe, G. W.; Ziller, J. W. *Organometallics* **1994**, *13*, 1641.
(9) Evans, W. J.; Shreeve, J. L.; Boyle, T. J.; Ziller, J. W. *J. Coord. Chem.* **1995**, *34*, 229.
(10) Deacon, G. B.; Gitlits, A.; Skelton, B. W.; White, A. H. *J. Chem Soc., Chem. Commun.* **1999**, 1213.
(11) Deacon, G. B.; Gitlits, A.; Roesky, P. W.; Bürgstein, M. R.; Lim, K. C.; Skelton, B. W.; White, A. H. *Chem.—Eur. J.* **2001**, *7*, 127.
(12) Deacon, G. B.; Forsyth, C. M.; Gitlits, A.; Skelton, B. W.; White, A. H. *J. Chem. Soc., Dalton Trans.* **2004**, 1239.
(13) Müller-Buschbaum, K.; Quitmann, C. C. *Inorg. Chem.* **2003**, *42*, 2742.
(14) Müller-Buschbaum, K.; Quitmann, C. C. *Inorg. Chem.* **2006**, *45*, 2678.
(15) Müller-Buschbaum, K.; Mokaddem, Y. *J. Chem Soc., Chem. Commun.* **2006**, 2060.
(16) Müller-Buschbaum, K. *Z. Naturforsch.* **2006**, *61b*, 792.

10.1021/cm0619961 CCC: $37.00 
Published on Web 01/18/2007

**Table 1. Crystallographic Data for $^3_\infty$[Tb(Im)$_3$]@NH$_3$ (deviations given in brackets)**

| | |
|---|---|
| formula | $C_9H_{12}N_7Tb$ |
| cell constants (pm; deg) | $a = 666.75(8)$; $\alpha = 89.43(2)$ |
| $V$ ($\times 10^6$ pm$^3$) | 296.36(6) |
| $Z$ | 1 |
| $T$ (K) | 170 |
| $d_{calcd}$ (g cm$^{-3}$) | 2.253 |
| X-ray radiation | Mo−K$_\alpha$, $\lambda = 71.07$ pm |
| diffractometer | STOE IPDS II |
| cryst syst, space group | rhombohedral, $R3$ |
| BASF [18] | 0.4755(3) (racemic twin) |
| data range | $6.12 \le 2\theta \le 59.04$, $\Delta\Omega = 2°$, $\varphi = 0/90°$ $-9 \le h \le 9$; $-9 \le k \le 9$; $-9 \le l \le 9$ |
| no. of measured reflns (all) | 5584 |
| no. of unique reflns; $R_{int}$ (all) | 1093; 0.097 |
| no. of params | 52 |
| reflections:parameters ratio | 21 |
| abs coeff ($\mu$/cm$^{-1}$) | 59.7 |
| $R_1$[a] for $n$ reflections with $F_o > 4\sigma(F_o)$; $n$ | 0.042; 1093 |
| for all reflections | 0.042 |
| $wR_2$[b] (all) | 0.097 |
| remaining elec. density (e/pm $\times 10^6$) | +1.6/−1.7 |

[a] $R_1 = \sum[F_o - F_c]/\sum[F_o]$; [b] $wR_2 = (\sum w(F_o^2 - F_c^2)^2/\sum w(F_o^4))^{1/2}$.[18]

amalgam activation, imidazole (ACROS, 99%), and terbium metal (CHEMPUR, >99%) were used as purchased.

Tb metal (1 mmol) and imidazole (ImH, 4 mmol), together with Hg (0.2 mmol), were sealed in an evacuated DURAN glass ampule and heated to 155 °C in 7 h. The temperature was held for 72 h and then raised to 160 °C in another 50 h. This temperature was again held for 72 h and then raised to 165 °C in another 50 h. This temperature was held for 288 h. The reaction mixture was then constantly cooled to room temperature within 280 h. Except for an excess of the reactants and the activating Hg, the reaction was complete, resulting in highly reflective colorless crystals of the product. Yield: 212 mg = 55%.

Anal. Calcd for $C_9H_{12}N_7Tb$ ($M_w = 377.2$ g mol$^{-1}$): C, 29.34; N, 26.63; H, 3.26. Found: C, 29.5; N, 26.1; H, 3.2. MIR (KBr): 3414 mb, 3125 s, 2923 w, 1500 w, 1460 s, 1401 vs, 1330 w, 1308 m, 1250 w, 1229 s, 1137 m, 1108 m, 1072 s, 1063 ssh, 938 s, 850 m, 751 s, 675 s, 661 s cm$^{-1}$. FarIR (PE): 558 w, 494 w, 418 w, 351 w, 231 s, 220 msh, 186 m, 144 m, 71 m cm$^{-1}$. Raman: 3134 s, 3104 s, 1488 s, 1450 m, 1325 m, 1300 m, 1254 vs, 1141 vs, 1101 m, 450 s, 409 s, 142 vs, 93 vs cm$^{-1}$.

**Physical Measurements.** The best out of five single crystals of $^3_\infty$[Tb(Im)$_3$]@NH$_3$ was selected for single-crystal X-ray investigations under glovebox conditions and sealed in a glass capillary. The data collection was carried out on a STOE IPDS−II diffractometer at 170 K (Mo K$\alpha$ radiation $\lambda = 0.7107$ Å). The structure was determined using direct methods.[17] All non-H atoms were refined anisotropically by least-squares techniques.[18] All hydrogen positions were calculated into pre-set positions adjusting their thermal parameters to 1.2 of the referring carbon atoms. The crystal system and space group were checked proving them as the only reasonable choices (PLATON[19]). $^3_\infty$[Tb(Im)$_3$]@NH$_3$ crystallizes in the rhombohedral space group $R3$ as racemic twins (BASF: 0.4755(3)). Crystallographic data are summarized in Table 1. Further information was deposited at the Cambridge Crystallographic Data Centre, CCDC, 12 Union Road, Cambridge CB2 1EZ, UK (fax: 44 1223336033 or e-mail: deposit@ccdc.cam.ac.uk) and may be requested by citing the deposition number CCDC-618719, the names of the authors, and the literature citation.

The IR spectra were recorded using a BRUKER FTIR-IS66V-S spectrometer, the Raman spectra using a BRUKER FRA 106-S spectrometer. For MIR investigations, we prepared KBr pellets under vacuum; for FIR measurements, PE pellets. The thermal behavior was studied using simultaneous DTA/TG (NETZSCH STA-409). Therefore, both the bulk products of the melt reactions as well as products purified by washing excess ligand off with toluene were investigated. The bulk product of $^3_\infty$[Tb(Im)$_3$]@NH$_3$ (30.5 mg) and 20.9 mg of the crystalline product were heated from 20 °C up to 700 and 800 °C, respectively, at a heating rate of 10 °C/min in a constant Ar-flow of 60 mL/min. The thermal properties of the crystalline product were further investigated by mass spectrometry (BALZERS QMS 421 quadropole mass spectrometer, 0.2s scanning time per mass) simultaneously to DTA/TG. Signals (endothermic): mp of excess imidazole (85 °C), release of ammonia (4%, steady up to 180 °C), release of excess imidazole (200−310 °C), and decomposition of the network (640 °C).

Photoluminescence measurements on a crystalline sample at room temperature and 77 K were recorded on a Jobin-Yvon fluorescence spectrometer (Fluorolog 3) equipped with two 0.22 m double monochromators (SPEX, 1680) and a 450 W xenon lamp. The emission spectra were corrected for photomultiplier sensitivity, the excitation spectra for lamp intensity, and both for the transmission of the monochromators. Cooling to 77 K was achieved by the use of a nitrogen cryostat (Janis Research Co., VNF-100). Room-temperature reflection spectra were recorded with the aid of a Specord S100 spectrometer.

## Results and Discussion

**Synthesis**. Prevention of co-ligands by solvent free synthesis can be used as a tool for crystal engineering and formation of N-coordination networks of the lanthanides. To achieve reaction, the amine (imidazole) is used in molten state. The lanthanide metal is activated by an intermediate amalgam formation,[20,21] which further reacts with the amine melt to give the homoleptic amide network and hydrogen (for alternative lanthanide metal activation types, see ref 14). Simultaneously, the melt starts to decompose producing ammonia. The latter is found intercalated in cavities of the structure. The decomposition of the amine melt differs, for example, from aromatic *N*-heterocycles that contain neighboring nitrogen atoms and release $N_2$ instead of $NH_3$ in these kinds of reactions.[15] Consequently, with bridging ligands like imidazole, network structures can be achieved.

**Crystal Structure of $^3_\infty$[Tb(Im)$_3$]@NH$_3$.** $^3_\infty$[Tb(Im)$_3$]@NH$_3$ crystallizes in the noncentrosymmetric space group $R3$. Terbium is trivalent and coordinated by six N atoms forming nearly undistorted trigonal prisms (Figure 1). Compared to $^3_\infty$[Pr(Im)$_3$(ImH)]@ImH[16], the radii contraction[22] is evident, as pentagonal bipyramids are observed for Pr$^{3+}$. All ligand rings in $^3_\infty$[Tb(Im)$_3$]@NH$_3$ are imidazolate anions coordinating $\eta^1$ with their N atoms to different Tb ions. This results in a $\eta^1$:$\eta^1$ linkage that constitutes the three-dimensional network structure (Figure 2). The Tb−N distances are 240.3-

(17) Sheldrick, G. M. *SHELXS-97, Program for the Resolution of Crystal Structures*; Universität Göttingen: Göttingen, Germany, 1997.
(18) Sheldrick, G. M. *SHELXL-97, Program for theRefinement of Crystal Structures*; Universität Göttingen: Göttingen, Germany, 1997.
(19) Spek, A. L. *PLATON-2000, A Multipurpose Crystallographic Tool*; Utrecht University: Utrecht, The Netherlands, 2000.
(20) Magyar, B. *Inorg. Chem.* **1968**, *7*, 1457.
(21) *Gmelin Handbuch der anorganischen Chemie, Ergänzungsband der Seltenerdelemente*, Springer-Verlag: Berlin, 1978; Vol. 39, B6.
(22) Shannon, R. D. *Acta Crystallogr., Sect. A* **1976**, *32*, 751.

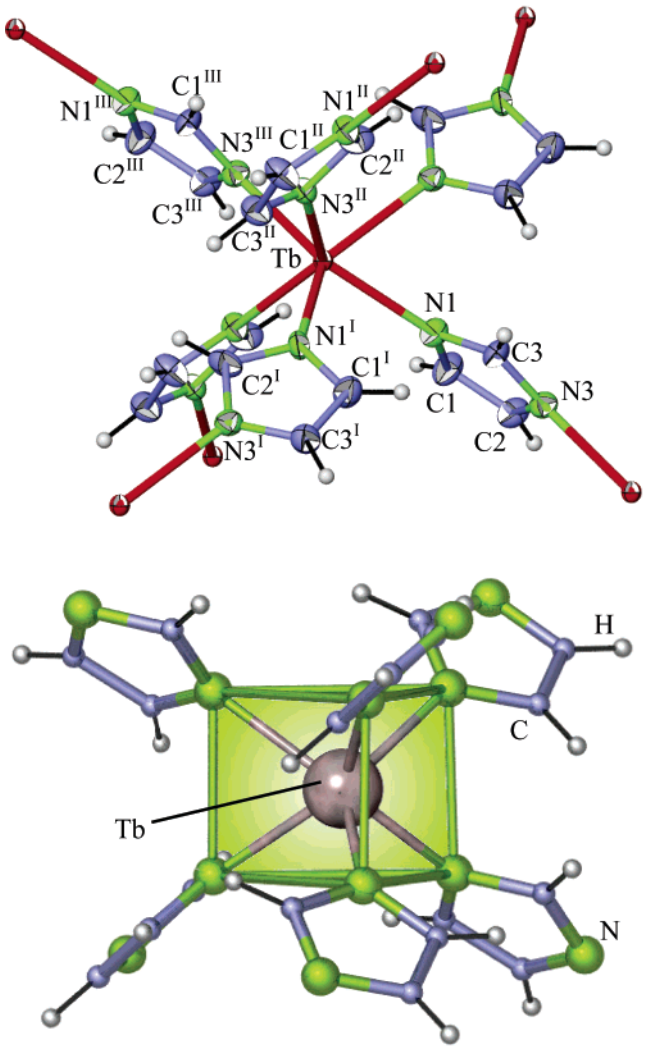


**Figure 1.** Coordination of $Tb^{3+}$ ions by imidazolate anions in the $^3_\infty[Tb(Im)_3]$ network of $^3_\infty[Tb(Im)_3]@NH_3$. The thermal ellipsoids (top) depict 50% of the probability level of the atoms. The coordination geometry is a nearly undistorted trigonal prism, which is highlighted by shading. H atoms are omitted for clarity (bottom). Symmetry operations: I *z*, *x*, *y*; II *x*, *y* + 1, *z*; III *z*, *x*, *y* + 1.

(9) and 214.6(9) pm and thus in the expected range for $Tb^{3+}$.[22] The N−Tb−N angles reveal that the trigonal prisms are nearly undistorted. For details on the crystal structure determination of $^3_\infty[Tb(Im)_3]@NH_3$, see Table 1, and for selected interatomic distances and angles, see Table 2.

As in $^3_\infty[Pr(Im)_3(ImH)]@ImH$[16], the network structure exhibits cavities. For praseodymium, these cavities are large enough to contain imidazole molecules. In $^3_\infty[Tb(Im)_3]@NH_3$, they are smaller and contain 1 equiv of ammonia each. These $NH_3$ molecules are not positioned in the centers of the cavities but orientated toward one C−H group of a neighboring imidazolate ring so that weak N−H bridging can be achieved. In both imidazolate networks, intercalated molecules can be thermally removed from the cavities, as the DTA/TG analysis reveals. For $^3_\infty[Tb(Im)_3]@NH_3$, the release of ammonia can also be observed over time if no outer ammonia pressure is provided. After 2 months, microanalysis shows that no ammonia remained. REM visualizations reveal the aged character of the crystals by hole formation visible on the surface.

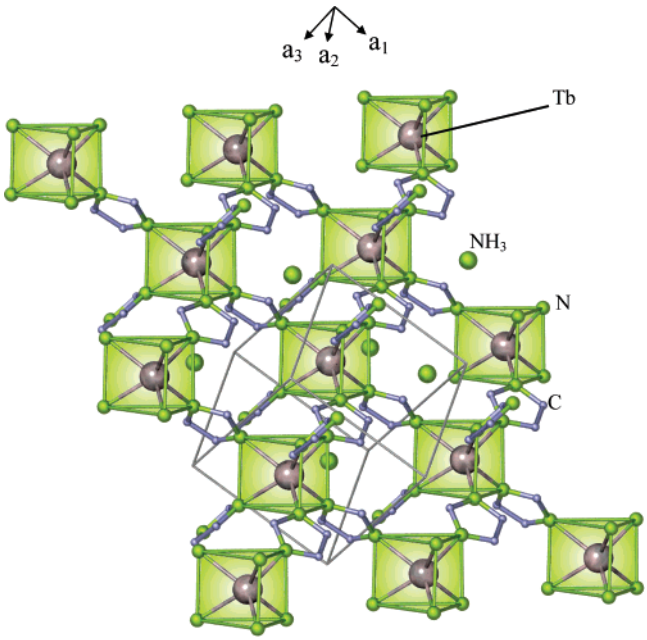


**Figure 2.** Crystal structure of $^3_\infty[Tb(Im)_3]@NH_3$ displaying the network structure as well as $NH_3$ intercalated into cavities of the structure. Both the unit cell and the coordination polyhedra are depicted. H atoms are omitted for clarity. The structure is noncentrosymmetric as all trigonal prisms point into the same direction.

**Table 2. Selected Interatomic Distances (pm) and Angles (deg) of $^3_\infty[Tb(Im)_3]@NH_3$ (deviations given in brackets)**

| distances | | | | angles | |
|---|---|---|---|---|---|
| Tb−N1 | 241.6(9) | N2−C2 | 136(2) | N1−Tb−N1$^{I}$ | 90.54(3) |
| Tb−N2 | 240.3(9) | N2−C3 | 139(2) | N2$^{II}$−Tb−N2$^{III}$ | 93.79(3) |
| N1−C1 | 135(2) | C1−C2 | 137(2) | N1−Tb−N2$^{II}$ | 67.44(3) |
| N1−C3 | 137(2) | N3−(N,C) | 318−329 | N1−Tb−N2$^{III}$ | 132.15(3) |

[a] Symmetry operations: I *z*, *x*, *y*; II *x*, *y* + 1, *z*; III *z*, *x*, *y* + 1.

**Photoluminescence.** $^3_\infty[Tb(Im)_3]@NH_3$ shows a strong green emission by irradiation with a UV lamp (255 nm), which is typical for $Tb^{3+}$-containing samples. However, the brightness is amazingly strong for a fully concentrated compound. On the other hand, the effect of concentration quenching for some phosphors is very small, e.g., $Tb_xLa_{1-x}P_5O_{14}$ has the highest emission intensity for $x = 1$.[23] Because the f−f transitions of lanthanide ions are forbidden and thus direct excitation would lead to a rather weak luminescence, the intensity in the present case points to a ligand excitation followed by an efficient ligand−terbium energy transfer (see below).

The emission as well as the excitation spectra at 77 K are depicted in Figure 3. In the emission spectrum, numerous small peaks are present that can be assigned to the intra-4f $^5D_4 \rightarrow {}^7F_J$ ($J = 2 - 6$) transitions of $Tb^{3+}$ ions. The dominant emission is located at 540.9 nm (18487 $cm^{-1}$), corresponding to $^5D_4 \rightarrow {}^7F_5$. This transition is extremely sharp (fwhm = 40 $cm^{-1}$) even in comparison to other Tb compounds,[23] which indicates a good color quality of the emission. Concerning this point of view, another advantage is that only the $^5D_4 \rightarrow {}^7F_{5,3}$ transitions have a large intensity, whereas $^5D_4 \rightarrow {}^7F_{6,4,2}$ transitions are rather weak. Moreover, the blue $^5D_3 \rightarrow {}^7F_J$ transitions, which are located at higher energies

(23) Shionoya, S.; Yen W. M. *Phosphor Handbook*; CRC Press: Boca Raton, FL, 1999.

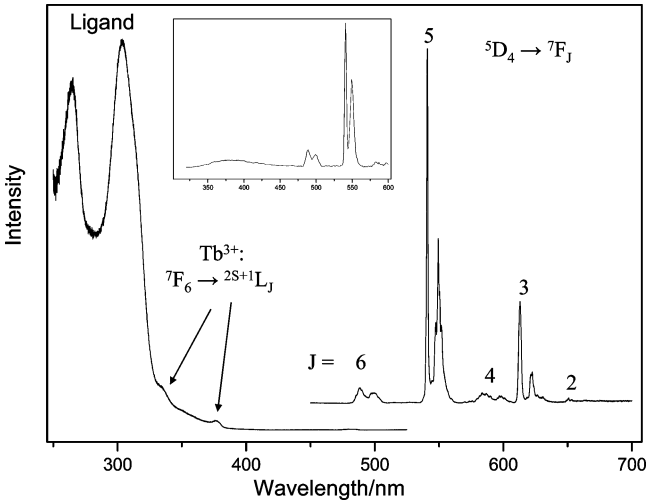


**Figure 3.** Photoluminescence spectra of $^3_\infty[Tb(Im)_3]@NH_3$ at 77 K. Left, excitation spectrum ($\lambda_{em} = 541$ nm); right, emission spectrum ($\lambda_{ex} = 306$ nm). The inset depicts ligand emission in relation to the $^5D_4 \rightarrow {}^7F_5$ emission intensity.

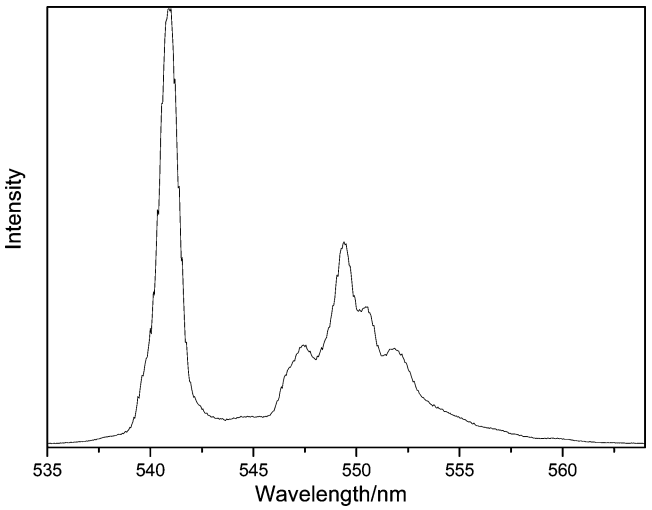


**Figure 4.** Section of the high-resolution emission spectrum of $^3_\infty[Tb(Im)_3]@NH_3$ at 77 K.

and would result in a bluish white emission as a sum, are not observed in the present case. This can be explained by the high $Tb^{3+}$ concentration, which causes an efficient cross relaxation ($Tb(^5D_3) + Tb(^7F_6) \rightarrow Tb(^5D_4) + Tb(^7F_0)$[24]). Some fine structure observed in each emission band is attributed to perturbation by the crystal field, although the Stark levels cannot be resolved because of their variety caused by the large $J$ values. The $^5D_4 \rightarrow {}^7F_5$ part of the emission spectrum recorded in high resolution (0.1 nm) is shown in Figure 4.

The excitation spectrum (Figure 3, left part) includes some small $Tb^{3+}$ f−f transitions ($^7F_6 \rightarrow {}^5L_{10}$ at 378 nm and $^7F_6 \rightarrow {}^5D_2$ at 335 nm) that can be clearly observed as sharp lines in a high-resolution spectrum with long averaging (not shown). Moreover, two broad excitation bands are detected with maxima at 265 nm (37740 $cm^{-1}$) and 304 nm (32 900 $cm^{-1}$) that can be assigned to transitions of the imidazolate ligands. Although we were not able to detect any fluorescence of pure imidazole, the respective reflection spectrum (not shown) shows two bands with comparable shape at 329 nm (30 400 $cm^{-1}$) and 385 nm (25 970 $cm^{-1}$). The shift to higher energies for the complex ligand transitions can be explained by the distortion of the planar $\pi$ system of free imidazole. The imidazolate emission can be seen as a weak broadband with a maximum at about 385 nm, and excitation of the ligand results rather in a strong $Tb^{3+}$ emissionm as is obvious from the inset in Figure 3. Thus, $^3_\infty[Tb(Im)_3]@NH_3$ shows an efficient ligand → $Tb^{3+}$ energy transfer, which causes the strong emission intensity. The transfer is probably from the triplet T1 state of imidazolate, because singlet energy transfer is very uncommon and was recently detected for the first time.[25]

The high excellence of the photoluminescence properties of $^3_\infty[Tb(Im)_3]@NH_3$ are also shown by comparison with those of other compounds containing Tb−N bonds. Also, strong luminescence is reported for $Tb[N(CN)_2]_3 \cdot 2H_2O$.[26] Although the excitation spectrum is somewhat shifted to lower energy compared to $^3_\infty[Tb(Im)_3]@NH_3$, large Tb 4f → 4f excitation bands are included in the excitation spectrum that are very weak in the present case. This indicates the advantage of the antenna effect, which is efficient excitation of an aromatic ligand followed by energy transfer. Moreover, the ratio $I(^5D_4 \rightarrow {}^7F_5)/I(^5D_4 \rightarrow {}^7F_J)$ is much larger for $^3_\infty[Tb(Im)_3]@NH_3$ compared to $Tb[N(CN)_2]_3 \cdot 2H_2O$, pointing to a better color quality.

As a result, it can be assumed that the luminescence properties can be further improved by tailoring the structure for this purpose. The respective $Gd^{3+}$ compound should have the same structure so that doping can be easily achieved. Furthermore, removal of the ammonia molecules or their substitution leads to the attractive possibility to optimize the emission intensity. Respective projects are under present investigation.

**Thermal Analysis, IR, and Raman Investigations.** To confirm the results of the X-ray single crystal analysis and the intercalation of ammonia molecules, we also investigated $^3_\infty[Tb(Im)_3]@NH_3$ by simultaneous DTA/TG/MS and IR and Raman spectroscopy.

The thermal analysis reveals the excess of imidazole from the melt synthesis in the bulk sample (see Figure 5), as both the melting point (85 °C, signal 1) as well as the boiling point of the free ligand ImH (255 °C, signal 3) are detected. As expected, imidazole is volatile prior to its boiling point and evaporated from the sample from 200 °C on (signal 2). Thus the melt synthesis has a yield of approximately 55%. The network itself is thermally highly stable and starts to decompose at 640 °C (signal 4). A steady decrease in the sample mass from the start of the analysis up to 180 °C is identified with the release of ammonia (4% recalculated on the basis of a 55% yield of the reaction). The low amount released together with the long time scale of 15 min prevent detection of a DTA signal. The interpretation is supported by the results of mass spectroscopy, revealing ammonia first ($m/z = 17, 16, 15$) followed by imidazole molecules ($m/z = 68$, fragments: 41, 38, 27) and ending up with the release

(24) Nakazawa, E; Shionoya, S. *J. Phys. Soc. Jpn.* **1970**, *28*, 1260.

(25) Yang, C.; Fu, L. M.; Wang, Y.; Zhang, J. P.; Wong, W. T.; Ai, X. C.; Qiao, Y. F.; Zou, B. S.; Gui, L. L. *Angew. Chem., Int. Ed.* **2004**, *43*, 5010.

(26) Nag, A.; Schmidt, P. J.; Schnick, W. *Chem. Mater*. **2006**, *18*, 5738.

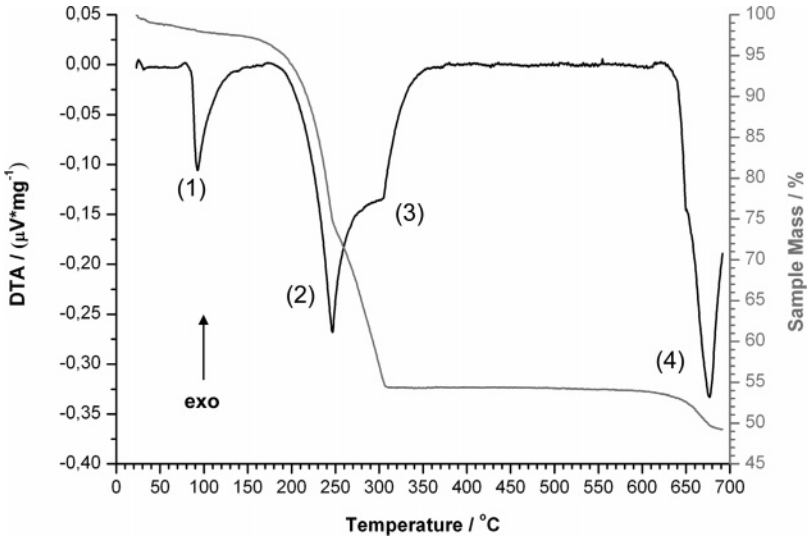


**Figure 5.** Simultaneous DTA/TG analysis of the bulk sample of $^3_\infty[Tb(Im)_3]@NH_3$ between 20 and 700 °C with a heating rate of 10 °C/min (Ar).

of fragments of the imidazolate anions ($m/z$ = 48, 44, 41, 38, 27, 17, 16, 15) upon decomposition of the network.

Besides the expected ligand bands of the imidazolate anions, the FIR and Raman spectra show bands that cannot be identified with the free ligand and indicate $\upsilon$(Ln-N) vibrations (FIR: 231, 220, 186, 144 $cm^{-1}$. Raman: 142, 93 $cm^{-1}$). The nearly undistorted trigonal prism of N atoms around the Tb center is responsible for $^3_\infty[Tb(Im)_3]@NH_3$ being Raman active and thus different from the less-symmetric distorted pentagonal bipyramidal coordination in $^3_\infty[Pr(Im)_3(ImH)]@ImH$, which does not show Raman bands in the referring region of wavenumbers.[16] The FIR bands match with those of the praseodymium network[16] as well as the expected region of other heterocyclic Ln amides.[1−6,13−15]

## Conclusions

Solvent-free reactions of molten amines with activated lanthanide metals can be utilized for the syntheses of dimensional as well as homoleptic rare earth amides. Selection of the lanthanide metals and respective *N*-heterocyclic amines are tools of crystal engineering as both influence coordination and structure of the amides. As for $^3_\infty[Tb(Im)_3]@NH_3$, 3D networks with complete nitrogen coordination can be obtained. As the lanthanide ions have large radii and prefer large C.N.s, prevention of coligands by solvent-free synthesis enforces a bridging coordination of the imidazolate rings. This leads to formation of a network structure. Network-related parameters like cavities and their extensions can be directed by the lanthanides used (and their radii). The presented compound possesses outstanding luminescence properties concerning the intensity and the color quality, which are the results of an efficient ligand excitation followed by energy transfer and high $Tb^{3+}$ concentration. The possibility of crystal engineering leads to a system with the chance of optimizing the optical properties for luminescent materials.

This paper is dedicated to Professor Josef Hahn on the occasion of his 65th birthday. We thank the Deutsche Forschungsgemeinschaft for funding this work through the Schwerpunktprogramm 1166 “Lanthanoid-spezifische Funktionalitäten in Molekül and Material”. K.M.-B. and S.G.-T. are also grateful to Prof. Dr. G. Meyer, Institut für Anorganische Chemie, Universität zu Köln, for his generous support.

CM0619961